Int J Adv Manuf Technol (2015) 77:653–661
DOI 10.1007/s00170-014-6486-z

ORIGINAL ARTICLE

Optimization for radial knurling connection process of assembled camshaft using response surface method

Peng Zhang · Shuqing Kou · Baojun Lin · Yumei Wang

Received: 12 July 2014 / Accepted: 7 October 2014 / Published online: 21 October 2014

Abstract In the present paper, an optimization of radial knurling connection process of assembled camshaft has been carried out using response surface methodology (RSM) and finite element simulation analyses based on the coupled Euler–Lagrange (CEL) algorithm. In order to evaluate the simulation results, corresponding experiments are implemented. The challenge in optimizing the connection process is to increase static torsional strength and, at the same time, to decrease press-fit load, thus static torsional strength and press-fit load are the objective functions taken into account. The tooth height, tooth angle, and feed, which all have decisive influences on the objective functions, are regarded as independent variables. The optimization results are the key references to design knurling cutters and assembled machines. The conclusion of this study is that the simulation and experimental results are highly consistent and the response model possesses high predictive ability. There exists a group of optimal independent variables under confined conditions.

Keywords Assembled camshaft · Press-fit load · Static torsional strength · Numerical simulation · RSM optimization

1 Introduction

The recent developments of engine are high power, low fuel consumption, low emissions, lightweight, etc. The camshaft as a key part of the engine components and a core part of valve mechanism bears periodic impact load and dynamic torque increasingly. Owing to limitation of process and single material, the traditional camshaft which is produced by casting or forging is difficult to meet the new requirements. A new assembled camshaft has obvious advantages in reducing product weight and costs, improving production efficiency, material optimization, flexible design, and manufacturing. So it has outstanding market competitiveness and technical predominance [1–3]. The key technique of assembled camshaft production is connection process. The common connection methods are shrink fit, welding, powder sintering, knurling connection, and expanding tube joint [4]. The requirements of equipment for the former three connections are high, and they are easy to cause heat deformation that affect the assembled precision. So the rest are the main connection methods. Over the last 10 years, many investigation studies have been accomplished to the main connection. Blanchard and the others made the powder metallurgy CAM piece and shaft tube assembled together through the mechanical expanding. The tests showed that static torsional strength was 260 Nm and torsion fatigue strength was 210 Nm [5]. Liu et al. developed a six-cylinder diesel engine camshaft by using hydraulic bulging method and carried out the static torsional strength and fatigue strength tests on the specimens [6]. Kou and Zhang studied expanding tube connection technology to analyze the residual pressure and the strain distribution by the numerical simulation method [7, 8]. Kou and her co-workers analyzed factors of the axial knurling press-fit load and connection strength. The results pointed out that the main factors were the material, the amount of interference, and the length of knurling connection zone [9]. The knurling connection methods included axial and radial knurling connection. The former method applied to the assembly showed that the tube is harder than the cam and the latter is opposite. Typically, the cam should have pitting corrosion resistance and wear resistance and be harder than the tube. Experience shows that the radial knurling assembled technology is more applicable; however, research in the field is nearly blank. Press-fit load and static torsional strength are the two important indicators to measure the

P. Zhang · S. Kou (✉) · B. Lin · Y. Wang
Roll Forging Research Institute, Jilin University, Changchun 130025, China
e-mail: Kousq@jlu.edu.cn

quality of radial knurling assembly. However, there is a contradiction between them. With the connection reliability enhanced, the press-fit load increases accordingly which may lead to bending of the tube and even to sudden splitting of the cam, thereby affecting the assembled precision and the qualified rate of products. At the same time, the energy consumption may raise significantly. In this study, numerical simulations combined with design of experiments (DOEs) have been carried out in order to build basic quantitative relationship between independent variables and the optimal objectives with experimental verification as a supplement. Then, response surface methodology was presented for further optimization with the results from the simulation.

2 Radial knurling connection process and modeling

2.1 The connection process of radial knurling

The procedures of knurling connection include knurling and press-fit. The knurling cutters are used to roll a triangular tooth which is perpendicular to the axis. Then, the cam is pressed into the tube body individually with a certain amount of interference at room temperature (as shown in Fig. 1). Because the speed of press-fit is slow and tube material has great plastic flow capacity, concave–convex mosaic is formed like spline connection in the press-fit region [10]. And, the interference fit is generated in the tube and cam contact area tightly because of elastic deformation and rebound [11]. Therefore, as shown in Fig. 2, the composite connection can provide both shear and friction resistance. So the connection strength is greatly improved compared with the common interference joints [12].

Main factors which influence the press-fit load and static torsional strength include the tube and cam materials, the length of connection region, the amount of interference, and the knurling cutter parameters (tooth height, tooth angle). Actually, materials for a certain camshaft are usually given. Besides, press-fit load and connection strength are always positively correlated with the connecting region length determined by cam thickness. So further discussion on these issues is not necessary. The amount of interference is determined by the knurling cutter parameters and the amount of feed together. When knurling cutters with different tooth height feed uniformly to tube, knurling cutters with small tooth height may feed excessively which causes tooth damage, while a large one may feed insufficiently which causes tooth incomplete. In the actual knurling processes, different knurling cutters feed to tube with the same time and feeding force, and the ratio between amount of feed and tooth height is almost consistent. Therefore, the ratio is introduced to replace absolute amount of feed, which is also called feed. So the final independent factors are knurling cutter parameters (tooth height, tooth angle) and feed. They definitively mold the tooth profile on the surface of the tube and further affect the press-fit load and static torsional strength.

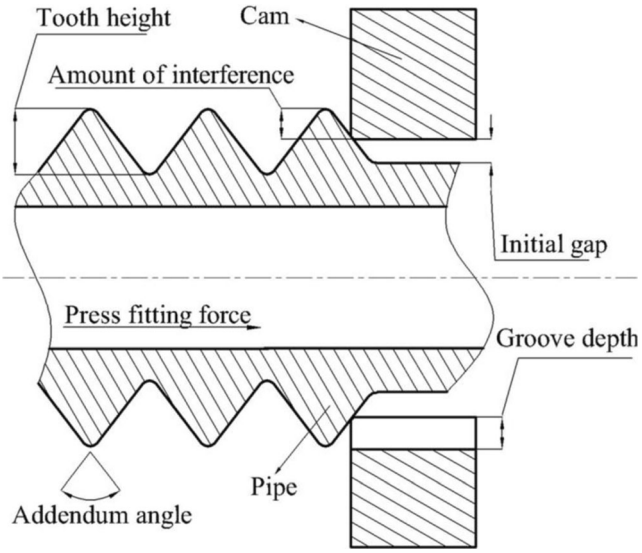

Fig. 1 Axial section of press-fit process

2.2 Mesh dependency of the CEL method

Because the knurling and press-fit processes involve large deformation, the use of classical finite element (FE) numerical methods which are based on the Lagrangian formulation often results in contact problems and the FE mesh distortion. To solve these problems, the CEL which is applied to extreme deformation comes into consideration.

In a conventional Lagrangian analysis, nodes are fastened with the material; meanwhile, elements deform as the material

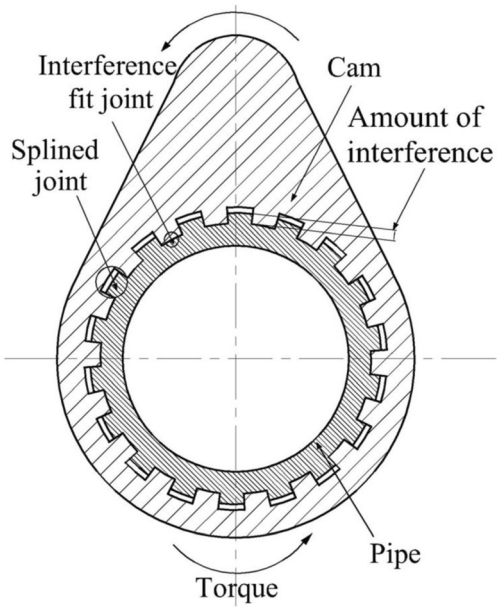

Fig. 2 Radial section of connector

deforms, so the material boundary accords with the element boundary. By contrast, in an Eulerian analysis, nodes are fastened in space, and material moves through elements which do not deform. Eulerian elements may not always be 100 % filled with material and many may be partly or afond void [13]. In numerical analyses, Eulerian volume fraction (EVF) is introduced to track material as it flows through the mesh. By computing EVF, each Eulerian element is designated a percentage, which represents the portion of that element filled with materials [14]. If an Eulerian element is completely filled with materials, its EVF is 1; if there is no material in the element, its EVF is 0. The eight-noded linear multi-material brick element with reduced integration is the only available Eulerian element in Abaqus. Eulerian mesh should be constructed to extend enough beyond the boundary of Eulerian material, and as shown in Fig. 3, the Eulerian domain is modeled material-free (void) at the beginning of the simulation to contain the soil material as it deforms outside the tube, and the domain is filled with soil material inside the tube. If any Eulerian material oversteps the Eulerian mesh, it disappears from the simulation.

2.3 Geometry model

Taking an automobile camshaft as a typical part, the knurling, press-fit, and torsional test processes were analyzed systematically with the numerical simulation so that the displacement and stress field can be passed from the previous step to the next step which is in order to retain hardening effect and improve simulation accuracy.

The camshaft was produced by connecting cam to tube sequentially. The connection process was repeated several times, usually eight times, to obtain a complete one. Each connection process was same, and there was almost no mutual influence on whatever adjacent steps. In this case, we can choose just a single process to simulate and analyze. The cam outline is like a peach in shape and is supposed to be very complex. The thinnest part of cam has greatly impacts on the connection process so the cam can be simplified into a thick wall cylinder. The wall thickness is the thinnest place of cam. Because of the symmetry in mechanics and shape, only a third of the tube and cam along the circumference needs to be modeled during simulation that is illustrated in Fig. 3. After numerical simulation of knurling process, the displacement and stress fields of the tube are regarded as the initial field for press-fit process. The geometry model of press-fit process is showed in Fig. 4. Finally, the tube is fixed and the cam is exerted torque in torsion simulation [15, 16].

2.4 Materials and other parameters

Geometrical properties and material properties of the cam and the tube are shown in Tables 1 and 2 which are all derived

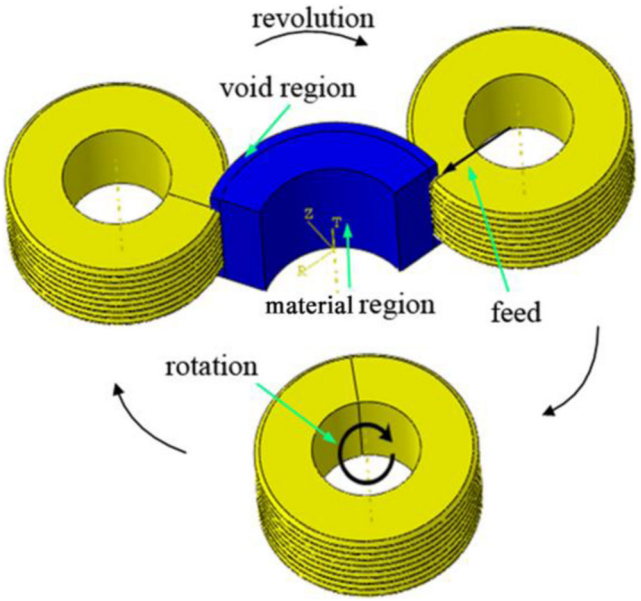

Fig. 3 Geometry model of knurling

from the typical automotive camshaft. Cam is the Fe–Cu–C-based powder metallurgy material with high hardness, which only presents elastic deformation in the main, but the stress concentration area may be prone to crack initiation. The tube is a kind of cold drawn seamless steel tube with thermal refining whose material is 16 Mn. The plastic deformation data used in simulation is obtained from single tensile tests. Knurling cutters were regarded as rigid bodies. The initial assembled clearance between the cam and tube is 0.1 mm, which can make the tube to insert into the cam smoothly to avoid scratches.

The metal of the tube complied with the kinematic hardening rule under repeated loading and unloading conditions. The knurling process referred to cold rolling without lubrication,

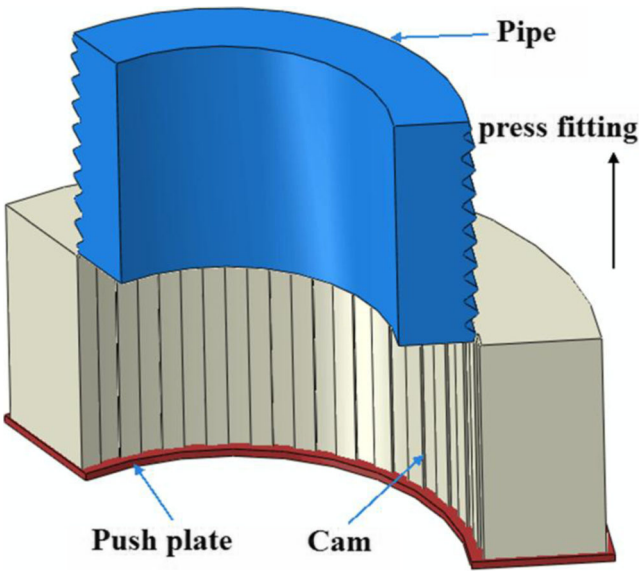

Fig. 4 Geometry model of press-fit

Table 1 Geometrical properties of the tube and cam

Part	Inner diameter (mm)	Outer diameter (mm)	Thickness (mm)
Cam	25.7	39	12.35
Tube	18	25.5	

and the coulomb friction coefficient is 0.11 [17]. Friction coefficient of press-fit and static torque processes is 0.125, which referred to interference fit without lubrication but plastic deformation [18].

3 Comparison of simulation and experiment

A common knurling cutter (tooth height=0.68 mm, tooth angle=75°) with feed=60 % was selected to carry out knurling experiments and simulations. The actual knurling processes [19] were completed in the self-developed CNC-assembled machine, and the knurling device is shown in Fig. 5. Figure 6 shows comparisons between the equivalent strain nephogram after knurling and radial section of experimental knurling area on the tube surface. The results have showed that the tube deformation of the experiment and the simulation are very similar. The deformation only appears on the surface of the tube.

Figure 7a shows the equivalent stress nephogram of the connection area, and Fig. 7b displays the deformation of the experimental connection area after press-fit on the tube surface. The simulation model takes only 15° along circumference from the experimental model. The press-fit experiments were performed on CSS-44100 electronic universal testing machine with the speed of 2.5 mm/s. As shown, the pressure stress of tube surface can reach up to 610 MPa, which evinces the high connection reliability.

Figure 8 presents the camshaft torque samples which were taken from the camshaft after press-fit. The destructive torsional experiments were performed in a QD-B1 static torsional test bench. The maximum value of torsion curve was the static torsional strength of camshaft.

Table 3 shows that the relative error of the experiment and simulation results is in an acceptable range. As a result, the numerical simulation could replace the actual experiments to analysis and optimize the whole processes with high credibility.

Table 2 Material properties of the tube and cam

Part	υ	E	ρ (g/cm^3)	σ_s (MPa)	σ_b (MPa)	HRC
Cam	0.27	160,000	7.1	680	705	14
Tube	0.30	210,000	7.85	350	720	56

Fig. 5 Knurling device

4 Optimization procedure

4.1 Bi-objective response surface methodology

Response surface methodology (RSM) consisted of mathematical and statistical methods provides an approximate relationship between a true response and design variables. The approximations are based on functional evaluations at selected points in the design space. RSM principles are applied to optimize a set of actual simulations presented by DOE to

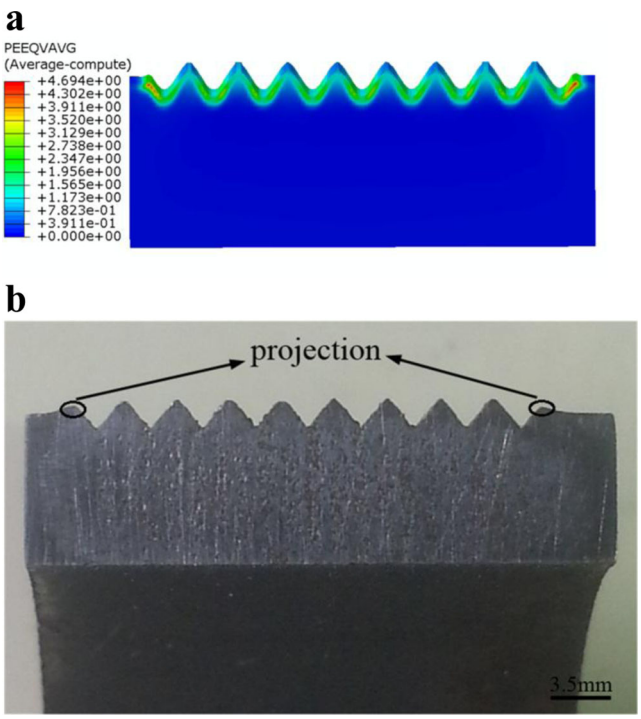

Fig. 6 Figure of knurling tooth profile. **a** Equivalent strain nephograms. **b** Actual radial section of knurling area

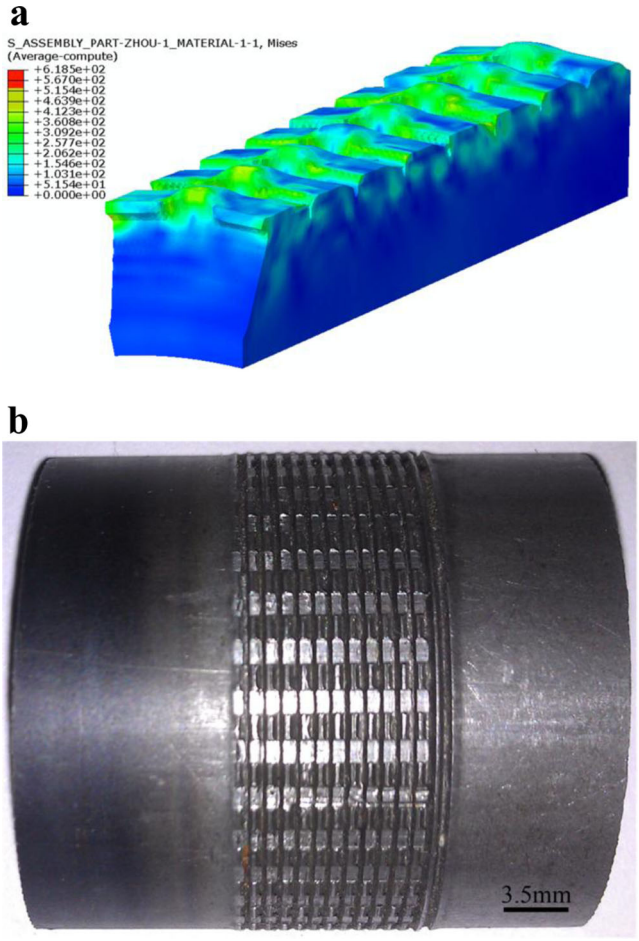

Fig. 7 Surface of the tube connection area. **a** Equivalent stress nephogram. **b** Actual deformation

achieve a template for purposed response. One of the most applicable and prosperous RSM tools is the central composite design (CCD). The next step in RSM is to find a suitable approximation for the true functional relationship between y and set of independent variables employed [20, 21].

Fig. 8 Samples of torsion test

Usually, a second order model is utilized in RSM which is only suitable for the single-objective optimization problem. In this study, the optimization targets include the press-fit load and static torsional strength, which belongs to the multi-objective optimization [22]. Especially, the "unification object method" is introduced to solve the multi-objective optimization, the usage of which is as follows: (1) every sub-objective is translated into dimensionless and equal-level numbers; (2) according to the importance of each sub-objective, they are weighting processed and combined into a uniform target function, which is detailed as follows:

Supposing that there are m objectives needed to be optimized and each one is denoted as $f_i(x)$, according to the technical requirements and numerical simulation results, the range of each objective is predicted and can be stated as follows:

$$\alpha_i \le f_i(x) \le \beta_i \quad (i = 1, 2, \ldots\ldots m) \tag{1}$$

In order to standardize the design objectives, each $f_i(x)$ is converted as follows:

$$f_{ti}(x) = \frac{f_i(x) - \alpha}{\beta_i - \alpha_i} \quad (i = 1, 2, \ldots\ldots m) \tag{2}$$

Obviously, $0 \le f_{ti}(x) \le 1$, so the unification function can be written as follows:

$$f(x) = \sum_{i=1}^{m} \omega_i f_{ti}(x) \quad (i = 1, 2, \ldots\ldots m) \tag{3}$$

where ω_i is the weighting coefficient. In Eq. 4, two optimization goals that are static torsional strength and press-fit load are denoted by T_s and P_f, respectively. The weighting coefficients are ω_1 and ω_2 separately.

$$f(x) = \omega_1 T_s - \omega_2 P_f \tag{4}$$

$$f(x) = 0.7 T_s - 0.3 P_f \tag{5}$$

The selection of weighting coefficients obeyed the following reasons:

1. After getting the unified objective function, the optimal parameter combinations could be obtained by means of calculating the maximum of the function, while the value of press-fit load should be as small as possible. So its coefficient was negative.

Table 3 Experiment and simulation results

	Tooth height (mm)	Press-fit load (kN)	Static torsional strength (Nm)
Simulation	0.248	13,158	405
Experiment	0.269	14,584	445
Relative error	7.8 %	8.6 %	8.9 %

2. Static torsional strength is one of the most important values to measure the connection strength of radial knurling connection. It is more difficult and important to increase static torsional strength than to decrease the press-fit load. So the static torsional strength should choose the bigger weighting coefficient.
3. The response surface optimization was actualized with three groups of weighting coefficient. The optimization results are listed in Table 4. As shown in Table 4, compared with the figures in the first group, the static torsional strength and press-fit load increased by 10 and 4 %, respectively, in the second group. And, the figures increased by only 3 % and no fewer than 8 %, respectively, in the third group based on the second group. So the weighting coefficient in the second group is more reasonable. The final unification function is depicted in Eq. (5).

4.2 Experimental design

As indicated in Sect. 2, all data for the optimization are derived from simulation instead of tedious experiments. Before the design, preparations are as follows: (1) the range of influence parameters is confirmed; (2) central composite design (CCD) is used to determine the level of each influencing parameters [23], which can avoid isolated experimental points and cover the best experimental condition.

The ranges of tooth height (H), tooth angle (a), and feed (F) were confirmed by the production experience, and then, their levels chosen are arranged in Table 5.

The final experimental design scheme was set up by CCD; then, the design results were simulated seriatim, so as to get the press-fit load and static torsion strength. The results were dealt with unification and weighting obeyed in Eqs. (2) and (5), which are listed in Table 6.

Table 4 Optimization results with different weighting coefficients

No.	ω_1	ω_2	Static torsional strength (Nm)	Press-fit load (N)
1	0.5	−0.5	391	8,919
2	0.7	−0.3	430	9,276
3	0.9	−0.1	443	10,093

5 Result and discussion

The least squares regression was applied to analyze the data in Table 4 to obtain the second-order response surface model:

$$Y = 0.31137 - 0.048962H + 0.0475\alpha + 0.053713F - 0.12757H^{*}F + 0.050952\alpha^{2} - 0.05026F^{2} \quad (6)$$

Analysis of variance was used in regression model in order to evaluate whether the model is valid. The analysis results are given in Table 7.

The significance of each term can be determined by "P value," which is listed in Table 7. If the P value of term is less than 0.05, it has a significant impact on the model. Otherwise, it has no significant effect and can be removed. As shown in Table 7, the linear terms a, b, and c; square terms A2 and B2; and cross term BC have P value less than 0.05, all of these have significant effects on the model.

The P value of the lack of fit is greater than 0.05, so the proportion of non-normal relative errors is small in model fitting. Except P value tests, statistic S and R^2 are also used to test the fitting degree of regression models [24]. The fitting degree R^2 is up to 83.05 %, which indicates that the model can reflect the response relationship between response value Y and independent variables (A, B, C) with satisfactory accuracy [25].

In this study, the requirement of static torsion strength for the typical automotive camshaft was no less than 200 Nm, which was introduced to be a constraint condition for the model. The multi-objective optimization mathematical model for press-fit load and static torsional strength of radial knurling connection is as follows:

Table 5 Level design of the variables

Variables	Levels				
	$-r$	Low	Zero	High	r
H (mm)	0.53	0.60	0.71	0.82	0.90
α (rad)	0.96	1.13	1.39	1.65	1.83
F	0.40	0.45	0.53	0.60	0.65

Table 6 Experimental layout and results

Run no.	Actual setting value			Y
	H	α	F	
1	0.60	1.13	0.45	0.2265
2	0.60	1.65	0.45	0.0064
3	0.82	1.13	0.45	0.5314
4	0.82	1.65	0.45	0.4577
5	0.60	1.13	0.60	0.3726
6	0.60	1.65	0.60	0.5348
7	0.82	1.13	0.60	0.4585
8	0.82	1.65	0.60	0.1845
9	0.71	0.96	0.53	0.4849
10	0.71	1.84	0.53	0.3285
11	0.53	1.40	0.53	0.2830
12	0.90	1.40	0.53	0.3763
13	0.71	1.40	0.40	0.0000
14	0.71	1.40	0.65	0.2409
15	0.71	1.40	0.53	0.2920
16	0.71	1.40	0.53	0.2930
17	0.71	1.40	0.53	0.2960
18	0.71	1.40	0.53	0.2910
19	0.71	1.40	0.53	0.2893
20	0.71	1.40	0.53	0.2896

$$\begin{cases} \text{Variables} & H\ ,\ \alpha\ ,\ F \\ \text{Maximum value} & Y = 0.7T_s - 0.3P_f \\ \text{Subject to} & 200 \le T_s \\ \text{Within the ranges} & 0.54 \le H \le 0.82 \\ & 1.14 \le \alpha \le 1.65 \\ & 0.45 \le F \le 0.60 \end{cases}$$

The forecast optimal results were obtained by solving the above equations, which are presented in Table 8. It is satisfied that the static torsional strength was as large as possible and the press-fit load was less meanwhile. Comparisons between the numerical simulation and the model forecast results were conducted to estimate the accurateness of the proposed model. The relative error is 6.17 % (press-fit load) and 5.3 % (static torsional strength), respectively, which are all in the authorized bound (as shown in Table 8) which is mainly from multivariate nonlinear regression calculation. Therefore, the improved mathematical formula for the bi-objective model had the satisfied prediction capability.

Table 8 Optimal independent variables and predicated values of the model

Tooth height (mm)	0.8
Tooth angle (°)	65
Feed	0.55
Press-fit load (RSM predict, N)	9,276
Press-fit load (simulation result, N)	9,886
Relative error (%)	6.17
Static torsional strength (RSM predict, Nm)	430
Static torsional strength (simulation result, Nm)	454
Relative error (%)	5.30

The 3D surface graphs of the bi-objective are displayed in Fig. 9. It is obvious from Fig. 9a that response Y is enhanced at the time when the tooth height is increased. When the height is lower than 0.67, the response can be reduced to 0.3 or so. The response Y tends to increase and then slightly decrease with the increase of tooth height. The reason is that the tooth angle increases initially, which leads to increment in the connection area. But, a further improvement in tooth angle results in decrease of tooth density, which reduces the connection area. Figure 9b indicates that the response Y first increases then decreases with the improvement in tooth height and feed. Figure 9c points out that, with an increase in the amount of feed, the response Y first increases and then decreases because the overlarge amount of feed destroys the roll teeth on the surface of the tube. With high press-fit load, the static torsional strength does not continue to increase instead of decrease.

Table 7 Analysis of variance for response surface quadratic model (response: the press-fit load and static torsional strength)

Source	Sum of squares	*df*	Mean square	*F* value	*P* value
Tooth height (A)	0.0338	1	0.0338	6.95	0.0333
Tooth angle (B)	0.0317	1	0.0317	6.66	0.0402
Feed (C)	0.0399	1	0.0399	7.96	0.0187
BC	0.1307	1	0.1307	21.68	0.0003
A^2	0.0384	1	0.0384	7.71	0.0207
C^2	0.0373	1	0.0373	7.56	0.0217
Residual	0.0262	13	0.0003		
Lack of fit	0.0262	8	0.0020		0.0787
Total	0.3961	19			

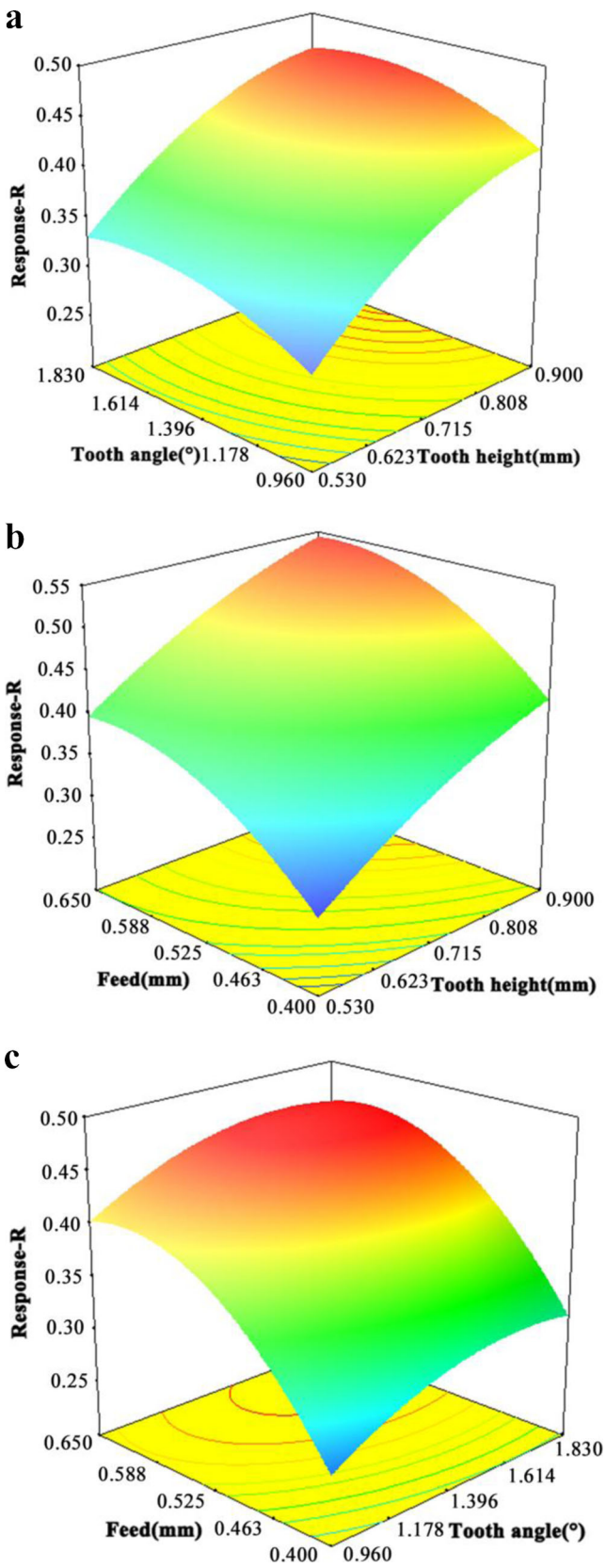

Fig. 9 3D surface graphs. **a** The interaction effect of tooth height and tooth angle at feed=52.5 %. **b** The interaction effect of tooth height and feed at tooth angle=80°. **c** The interaction effect of tooth angle and feed at tooth height=0.71 mm

6 Conclusions

The influencing parameters which effected on the radial knurling connection of assembled camshaft were analyzed quantitatively by the means of numerical simulation and RSM analysis. Based on the analysis and experimental verification, the following conclusions were drawn:

1. The whole processes of radial knurling, press-fit, and torsion test were performed by numerical simulation with the CEL analysis method. The previous displacement field and stress field were positively transferred to the next step as the initial simulation field, which was in order to retain effectively the strain hardening state of the previous step and improve simulation accuracy. The results showed that the relative errors of roll extrusion tooth height, press-fit load, and static torsion strength, between the simulation and the corresponding experiment, were 7.8, 8.6, and 8.9 %, respectively. It is proved that the simulation can replace experiments to analyze the connection process quantitatively with high credibility.
2. Bi-objective quadratic response surface model was established. Variance analysis showed that the regression *P* values of linear, cross, and square terms were less than 0.05 %, all of which had a great effect on the model.
3. The prediction values from the model were highly consistent with simulation results. The precision was closed to 83.05 %, which indicates that the model had a good prediction performance. The results showed that the model had great guide significance for knurling connection and could save time and reduce the cost effectively.
4. RSM was competent for solving the press-fit load and static torsional strength which is conflicting bi-objective optimization problem. In this paper, it is concluded that the optimal combinations of the independent variables including tooth height, tooth angle, and feed are 0.8 mm, 65°, and 55 %, respectively. The corresponding press-fit load and static torsional strength are 9,886 N and 454 Nm, respectively. The results have shown a significant improvement in working efficiency and connection quality.

Acknowledgments This research work was co-supported by The International Scientific and Technological Cooperation and Exchange Fund (No. 2011DFR70350) and the "Advanced CNC Machine Tools and Basic Manufacturing Equipment" Major Science and Technology Project (No. 2012ZX0409011).

References

1. Yang SH, Zang C, Kou SQ, Zhao Y (2004) Present status and trends of assembled camshaft technology. Chin Intern Combust Engine Eng 25:32–34

2. Deng ZH, Zhang XH, Liu W, Cao H (2009) A hybrid model using genetic algorithm and neural network for process parameters optimization in NC camshaft grinding. Int J Adv Manuf Technol 45:859–866
3. Mouton S, Ledoux Y, Teissandier D, Sebastian P (2011) Composite part design based on numerical simulation of the manufacturing process. Int J Adv Manuf Technol 55:421–431
4. Przybylski W, Wojciechowski J, Klaus A, Marre M, Kleiner M (2008) Manufacturing of resistant joints by rolling for light tubular structures. Int J Adv Manuf Technol 35:924–934
5. Blanchard P, Nigarura S, Trasorras JRL, Wordsworth R (2000) Assembled camshaft with sintered cam lobes: torsional fatigue strength and wear performance. Sae Tech Pap Ser 1:1–10
6. Liu Q, Liu G, Yuan SJ, Zhu SQ (2007) A hydro-joining assembled hollow camshaft and its joining strength measurement. Chin Intern Combust Engine Eng 28:67–71
7. Kou SQ, Zhang P, Han GM, Yang SH (2014) Connecting technology of multi-step tube expanding for assembled camshaft. J Jilin Univ (Eng Technol Ed) 44:398–403
8. Qiao J, Kou SQ, Kong QL, Qiao JY (2011) Analysis of hollow camshaft assembled process on expanding tube connection by pushing through a ball. J Jilin Univ (Eng Technol Ed) 41:115–120
9. Kou SQ, Qiao J, Pi WH, Yang SH (2008) Analysis of factors influencing knurling connected hollow camshaft assembling process. J Jilin Univ (Eng Technol Ed) 38:323–328
10. Zhang DW, Zhao SD (2014) New method for forming shaft having thread and spline by rolling with round dies. Int J Adv Manuf Technol 70:1455–1462
11. Luo Y, Wang XD, Wang MX, Tan DB, Zhang T, Yang YC (2013) A force/stiffness compensation method for precision multi-peg-hole assembly. Int J Adv Manuf Technol 67:951–956
12. Altinok M, Tas HH, Cimen M (2009) Effects of combined usage of traditional glue joint methods in box construction on strength of furniture. Mater Des 30:3313–3317
13. Abdolrahman D, Mohammad T, Shervani T, Boo CK (2011) A note on spark bubble drop-on-demand droplet generation: simulation and experiment. Int J Adv Manuf Technol 56:245–259
14. Al-Badour F, Merah N, Shuaib A, Bazoune A (2014) Thermo-mechanical finite element model of friction stir welding of dissimilar alloys. Int J Adv Manuf Technol 72:607–617
15. Ratchev S, Liu SL, Huang W, Becker AA (2007) Machining simulation and system integration combining FE analysis and cutting mechanics modeling. Int J Adv Manuf Technol 35:55–65
16. Qiu G, Henke S, Grade J (2011) Application of a Coupled Eulerian–Lagrangian approach on geomechanical problems involving large deformations. Comput Geotech 38:30–39
17. Wen BC, Huang WH, Tan JR et al (2010) Mechanical design manual 5. Machinery Industry Press, Beijing
18. Yang GM, Coquille JC, Fontaine JF, Lambertin M (2002) Contact pressure between two rough surfaces of a cylindrical fit. J Mater Process Technol 123:490–497
19. Lin BJ, Yang SH, Kou SQ, Hu BG (2012) Acceleration and deceleration control of assembled machine for assembled camshafts. Proc Inst Mech Eng B-J Eng Manuf 226:503–511
20. Montgomery DC (2001) Design and analysis of experiments, 5th edn. Wiley, New York
21. Cornell JA (1990) How to apply response surface methodology. American Society of Quality Control, Milwaukee
22. Zhang GJ, Zhang Z, Ming WY, Guo JW et al (2014) The multi-objective optimization of medium-speed WEDM process parameters for machining SKD11 steel by the hybrid method of RSM and NSGA-II. Int J Adv Manuf Technol 70:2097–2109
23. Kashiwamura T, Shiratori M, Yu Q (1997) Statistical optimization method. Comput Aided Optimum Des Struct 5:213–227
24. Palanikumar K (2008) Application of Taguchi and response surface methodologies for surface roughness in machining glass fiber reinforced plastics by PCD tooling. Int J Adv Manuf Technol 36:19–27
25. Xu XH, He MZ (2010) Experiment design and application of design-expert, SPSS. Science Press Beijing, Beijing